Energy & Environmental Science

ARTICLE

Optically transparent hydrogen evolution catalysts made from networks of copper-platinum core-shell nanowires†

Zuofeng Chen,[‡a,b] Shengrong Ye,[‡a] Adria R. Wilson,[a] Yoon-Cheol Ha,[a,c] and Benjamin J. Wiley[*a]

This article reports the fabrication of copper-platinum core-shell nanowires by electroplating platinum onto copper nanowires, and the first demonstration of their use as a transparent, conducting electrocatalyst for the hydrogen evolution reaction (HER). Cu-Pt core-shell nanowire networks exhibit mass activities up to 8 times higher than carbon-supported Pt nanoparticles for the HER. Electroplating minimizes galvanic replacement, allowing the copper nanowires to retain their conductivity, and eliminating the need for a conductive substrate or overcoat. Cu-Pt core-shell nanowire networks can thus replace more expensive transparent electrodes made from indium tin oxide (ITO) in photoelectrolysis cells and dye sensitized solar cells. Unlike ITO, Cu-Pt core-shell nanowire films retain their conductivity after bending, retain their transmittance during electrochemical reduction, and have consistently high transmittance (> 80%) across a wide optical window (300-1800 nm).

Broader context

Driven by the need to convert and store intermittent solar energy in chemical form, there has recently been a surge of activity to create an improved "artificial leaf" (*i.e.*, a photoelectrochemical cell, or PEC). An important consideration in the design of PECs is that the water splitting catalysts do not obstruct the transmission of light to the dye or photovoltaic component, but the design of highly active transparent catalysts for PECs has received relatively little attention. In addition, most PEC designs rely on the use of expensive indium tin oxide (ITO) as the transparent conductor. Here, we show that Cu-Pt core-shell nanowire (Cu_c-Pt_s NW) networks can serve as transparent, highly active catalysts, and eliminate the need for ITO.

Introduction

Solar-driven water splitting is an attractive means to convert intermittent solar radiation into H_2 for use as a storable, non-polluting fuel.[1-3] Photoelectrochemical cells (PECs), in which water splitting catalysts are directly connected to a dye or photovoltaic component, potentially offer lower fabrication costs compared to

systems composed of a separate photovoltaic module and electrolyzer.[4-6] An important consideration in the design of PECs is that the water splitting catalysts do not obstruct the transmission of light to the dye or photovoltaic component, but the design of highly active transparent catalysts for PECs has received relatively little attention.[1,7,8] Another impediment to the practical realization of PECs is that most designs rely on the use of indium tin oxide (ITO) as the transparent conductor. It has previously been estimated that the cost of a PEC must reach ~\$30 m^{-2} to be competitive with fossil fuels,[9] but the cost of ITO film by itself exceeds \$30 m^{-2}.[10] This cost arises from (1) the slow, vapor-phase sputtering process required to make high quality ITO film, (2) the fact that less than 30% of the ITO sputtered from a target ends up on the substrate, and (3) the low abundance of indium in the earth's crust.[11] ITO is also mechanically fragile and can become unstable at the potentials used for water splitting, losing its conductivity and transmittance.[12]

Copper nanowires (Cu NWs) are an attractive alternative to the high-conductivity ITO used in PECs because they can be deposited

[a] Department of Chemistry, Duke University, 124 Science Drive, Durham, North Carolina 27708, United States; Phone: (+1) 919-668-3066; E-mail: benjamin.wiley@duke.edu;
[b] Department of Chemistry, Tongji University, Shanghai 200092, China;
[c] Creative and Fundamental Research Division, Korea Electrotechnology Research Institute, Changwon 642-120, Korea.

‡ These authors contributed equally.

from solution at linear coating rates several orders of magnitude faster than ITO sputtering, offer nearly the same level of performance, and are composed of a material that is 1,000 times more abundant and 100 times cheaper than indium.[13-15] The fact that it is more energetically favorable for Pt to be on the surface of Cu rather than form an alloy also makes Cu NWs a promising electrocatalyst support material for this precious metal.[16] For example, Pt supported on Cu NWs has demonstrated greater mass activity and durability relative to Pt/C for oxygen reduction[17] and hydrogen oxidation[18]. However, the use of Cu-Pt NWs as a transparent conducting electrocatalyst has not been explored.

In this article we report the fabrication of Cu-Pt core-shell nanowire (Cu_c-Pt_s NW) networks by electroplating Pt onto Cu NWs, and their properties as an electrocatalyst for the hydrogen evolution reaction (HER) at neutral pH. In contrast to galvanic replacement, electroplating of Pt onto Cu allows the copper nanowires to retain their high conductivity, eliminating the need for a conductive support or overcoat of Nafion.[17-19] Cu_c-Pt_s NWs exhibit mass activities up to 8 times higher than carbon-supported platinum nanoparticles (Pt/C). At current densities equal to those obtained from an opaque polycrystalline Pt foil, films of Cu_c-Pt_s NWs exhibit a transmittance of > 75%. Cu_c-Pt_s NW films are also 10% more transparent than ITO when averaged across a wide optical window (300-1800 nm). Unlike ITO, Cu_c-Pt_s NW films retain their conductivity after bending, and retain their transmittance during electrochemical reduction. The superior properties of Cu_c-Pt_s NWs make them excellent candidates for use as transparent electrocatalysts in PECs, dye-sensitized solar cells (DSSCs), and spectroelectrochemical studies.[20-22]

Experimental

Chemicals. Sodium hydroxide was purchased from Fisher Scientific (S318-10). Copper(II) nitrate pentahemihydrate (12837), potassium hexachloroplatinate(IV) (379859), ethylenediamine (EDA, E1521), 35 wt% hydrazine (N_2H_4) in water (309400), *N, N*-diethylhydroxylamine (DEHA, 471593), polyvinylpyrrolidone (PVP, MW = 10,000), ethyl acetate (270989), pentyl acetate (109584), toluene (244511), and platinum on carbon (10 wt% Pt loading, Pt/C) were purchased from Sigma-Aldrich. Glass microscope slides (7.5 cm × 2.5 cm × 0.1 cm), polyethylene terephthalate (PET), and indium tin oxide (ITO) on glass (11 Ω sq^{-1}) or PET (42 Ω sq^{-1}) were purchased from McMaster-Carr. Nitrocellulose (712) was purchased from Scientific Polymer, and acetone, ethanol and isopropanol were purchased from VWR. All chemicals were used as received. Caution should be used when dealing with these chemicals as some are corrosive (highly concentrated NaOH), flammable (N_2H_4), or dangerous if ingested or put in contact with skin.

Synthesis of Cu NWs. Flasks and stir bars were cleaned with concentrated nitric acid, thoroughly rinsed with deionized water, and dried in an oven at 80 °C before use. Once dry, the flasks were allowed to cool to room temperature before any reactants were added.

Cu NWs were synthesized following a previously published procedure.[15] NaOH (20 mL, 15 M), Cu(NO$_3$)$_2$ (1 mL, 0.1 M), EDA (0.15 mL), and N_2H_4 (0.025 mL, 35 wt%) were added to a 50 mL round bottom flask. This mixture was swirled by hand for 5 seconds after each addition to mix the reactants. The solution was then heated at 80 °C and stirred at 200 rpm for approximately 3 minutes. After this heating step, the solution was poured into a 50 ml centrifuge tube, and a solution of PVP in water (5 ml, 0.4 wt%) was gently added to the top of the reaction solution. The centrifuge tube

containing the reaction solution was placed in an ice bath for 1 hour. The Cu NWs floated to the top of the reaction solution and were scooped into an aqueous wash solution containing N_2H_4 (3 wt%) and PVP (1 wt%). The wash solution containing the Cu NWs was centrifuged at 2,000 rpm for 5 minutes, and the supernate was decanted from the Cu NWs. The NWs were then dispersed in a new wash solution (containing 3 wt% N_2H_4 and 1 wt% PVP) by vortexing for 30 seconds, and then centrifuged and decanted for 3 more cycles. The Cu NWs were stored in a solution of N_2H_4 (3 wt%) and PVP (1 wt%) at room temperature to prevent oxidation.

Preparation of Cu NW Transparent Electrodes. Four 20 mL scale reactions were combined into one centrifuge tube after the initial washing steps. This suspension was centrifuged at 2,000 rpm for 5 minutes. The Cu NWs were washed 3 times using a solution of DEHA (1 wt%) containing no PVP to ensure that most of the PVP was removed. After the PVP was removed, the Cu NWs were washed with ethanol to remove the majority of the water and then washed once more with an ink formulation. The ink formulation was made by dissolving nitrocellulose (0.06 g) in acetone (2.94 g) and then adding ethanol (3 g), ethyl acetate (0.5 g), pentyl acetate (1 g), isopropanol (1 g), and toluene (1.7 g). After the Cu NWs were washed with the ink formulation, another portion of ink (0.3 mL) was added to the Cu NW precipitate, and this suspension was vortexed. The final concentration of Cu NWs in the ink formulation was approximately 8 mg mL^{-1}.

To prepare transparent Cu NW electrodes, glass microscope slides were placed onto a clipboard to hold them down while the Cu NW ink (30 µL) was pipetted in a line at the top of the glass slide. A Meyer rod (Gardco #13, 33.3 µm wet film thickness) was then quickly (< 1 second) pulled down over the Cu NW ink by hand, spreading it across the glass to form a thin, uniform film. The density of nanowires on the surface of the substrate could be adjusted by varying the concentration of the Cu NWs in the ink. The film was allowed to dry in air for 5-10 min followed by pressing with a shop press at a pressure of 80 bar for 1 min to lower the contact resistance between Cu NWs.

The Cu NW films were not conductive before being cleaned in a plasma cleaner (Harrick Plasma PDC-001) for 15 minutes in an atmosphere (forming gas) of 95% nitrogen and 5% hydrogen at a pressure of 600-700 mTorr to remove the nitrocellulose. The NW-coated glass samples were then heated at 175 °C in a tube furnace for 30 minutes under a constant flow of hydrogen (600 mL min^{-1}) to anneal the nanowires together and decrease the sheet resistance to its final value.[15]

Preparation of Cu_c-Pt_s NW Transparent Electrodes. Cu NW networks were coated with Pt by electroplating $PtCl_6^{2-}$ (0.1 mM) in 0.2 M deaerated phosphate buffer (pH 7.0) at room temperature. Electroplating was conducted by holding the potential at −0.30 V *vs.* NHE for different times to obtain different amounts of Pt on the NWs. To minimize galvanic replacement of Cu NWs by $PtCl_6^{2-}$, the Cu NW film was held at −0.30 V during the addition of K_2PtCl_6 to the solution. Cu_c-Pt_s NW networks were prepared on PET by following the same method.

For a control experiment, the Cu NW networks underwent galvanic replacement with Pt by dipping the Cu NW film into the same solution used for electroplating. In another control experiment, Pt/C was dispersed in an ethanol solution containing 0.05% Nafion to form a suspension with a Pt concentration of 0.1 mg mL^{-1}. A film of this catalyst was formed by pipetting 20 µL of this the catalyst suspension onto a 1 cm^2 of ITO-coated glass to reach a loading of 2.0 µg cm^{-2} of Pt.

2 | *Energy Environ. Sci.*, 2014, **00**, 1-7

This journal is © The Royal Society of Chemistry 2014

Characterization. The specular transmittance and sheet resistance of NW networks on glass or PET were measured using a UV/VIS spectrometer (Cary 6000i) and a four-point probe (Signatone SP4-50045TBS), respectively. Every reported value of the sheet resistance is the average of 5 measurements. The films were imaged with a dark field optical microscope (Olympus BX51) to show the density, distribution, and color of the nanowires in the film. To prepare the samples for SEM (FEI XL30 SEM-FEG), a small chip of NW film on glass or PET (5 mm × 5 mm) was placed on a piece of double sided conductive carbon tape on an SEM sample platform. The sample surface was then partially covered with carbon tape to electrically connect it to the platform, leaving a small spot uncovered for SEM imaging. To prepare the samples for bright field TEM (FEI Tecnai G² Twin), the NWs were carefully removed from the glass or PET by a razor and were dispersed in methanol by vortexing for 2 min followed by sonication for 2 seconds. Copper TEM grids with a thin coating of carbon (400 mesh, SPI, #3540C-FA) were used to support the nanowires. Once deposited on a grid, each sample was dried completely under a flow of nitrogen. The same sample preparation was performed for dark field TEM (FEI Titan 60-300 Aberration Corrected STEM) imaging and EDS mapping (Energy dispersive X-ray spectroscopy, Super X EDS System), except a silicon nitride grid (TEM windows, SN100-A10Q33B) was used. X-ray photoelectron spectroscopy (XPS) for elemental analysis was conducted on a Kratos Axis Ultra DLD X-ray Photoelectron Spectrometer. The carbon 1s peak (284.6 eV) was used for internal calibration.

To measure the concentration of the Cu NW suspension or the mass of the Cu NW film, a set volume of the suspension or a piece of as-prepared Cu NW film was dissolved in concentrated nitric acid (1 ml). The dissolved Cu NWs were then diluted to a set volume, and the concentration of Cu was analyzed using an atomic absorption spectrometer (AAS, Perkin Elmer 3100). To measure the mass percentage of Pt in Cu_c-Pt_s NWs, a piece of as-prepared Cu_c-Pt_s NW film was dissolved in aqua regia (1 ml). Cu and Pt concentrations were then measured by AAS.

To test the resistance of the NW networks to oxidation, the Cu and Cu_c-Pt_s NW films were stored in an oven at 85 °C for one month and their sheet resistance was measured periodically.

To test the flexibility of the Cu_c-Pt_s NW film on PET (thickness t = 0.1 mm), we attached one end of the film to a tabletop and the other end to a ruler which was on top of a spring. The set-up was designed so that the initial radius of curvature was r = 10 mm (no force applied to the ruler) and after a downward force was applied to the ruler the final radius of curvature was r = 2.5 mm. The ruler was then allowed to spring back to the starting position and the entire cycle was counted as 1. The sheet resistance was measured every 200 cycles. Error bars show one standard deviation for five measurements. The bending strain of the nanowire or ITO film on PET can be estimated by the following equation: $\varepsilon = t/2r$, with ε = 0.5% at r = 10 mm and ε = 2% at r = 2.5 mm.[23]

Electrocatalytic Water Reduction and Product Analysis. Electrochemical measurements were performed with the model CHI601D electrochemical workstation (CH Instruments, Austin, TX). The three-electrode system consisted of a working electrode, a coiled platinum wire as the counter electrode, and a saturated calomel reference electrode (SCE, ~0.244 V *vs.* NHE). Freshly prepared Cu_c-Pt_s NW networks with a geometric surface area of 1.5 cm² were used as the working electrode. Both CV and electrolysis measurements for catalytic water reduction were conducted under deaerated conditions. The amount of hydrogen evolved from electrolysis was measured by gas chromatography (GOW-MAC SERIES 600). Unless stated otherwise, all electrochemical experiments were conducted without stirring the solution, all potentials were reported *vs.* NHE without *iR* compensation, and all experiments were performed at 20 ± 2 °C.

Results and discussion

Fabrication and Characterization of Cu_c-Pt_s NW Networks. Figure S1 shows successive cyclic voltammograms (CVs) of a Cu NW film (30 Ω sq⁻¹, specular transmittance of 85% at 550 nm) in 0.2 M deaerated phosphate buffer (pH 7.0) containing 0.1 mM $PtCl_6^{2-}$. The electroplating of $PtCl_6^{2-}$ to Pt(0) on the nanowires is indicated by the increase in the current from hydrogen adsorption-desorption between −0.05 V and −0.30 V *vs.* NHE, as well as from hydrogen evolution. Coating the Cu NW networks with a thin layer of Pt was accomplished by holding the potential at –0.30 V. Figure 1A shows a typical electroplating curve for 30 min, as well as the Pt content of the Cu_c-Pt_s nanowires as a function of electroplating time. There was no significant effect on the rate of Pt electroplating by varying the applied potential from –0.20 V to –0.40 V.

Figure 1B shows that the transmittance of the NW networks gradually decreases with electroplating time as the thickness of the Pt coating increases. The sheet resistance of Cu NW networks increases slightly during the initial electroplating ($\leq$ 10 min). This is likely due to partial galvanic etching of the Cu NWs by $PtCl_6^{2-}$, which we discuss in further detail below. Additional plating of Pt after this initial stage does not appear to further increase the sheet resistance of the film. For a typical electroplating time of 10 min, the resulting Cu_c-Pt_s NW networks contain 9 mol% Pt, and exhibit a sheet resistance of 38 Ω sq⁻¹ at a specular transmittance of 83.4% (λ = 550 nm).
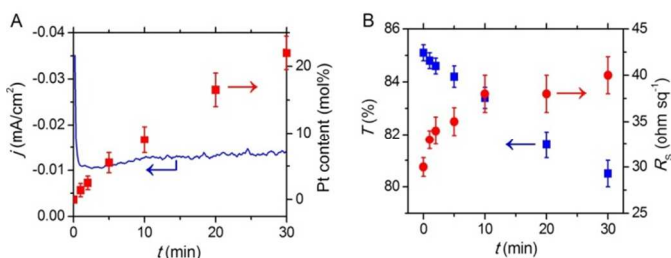

Figure 1. (A) Current and Pt content of the Cu NW film as a function of time during electroplating at –0.30 V *vs.* NHE. (B) Plots of transmittance (550 nm) and sheet resistance *vs.* electroplating time.

Figure 2 shows dark field optical microscopy (DFOM), scanning electron microscopy (SEM), transmission electron microscopy (TEM), and X-ray energy dispersive spectroscopy (EDS) images of Cu NW and Cu_c-Pt_s (9 mol% Pt) NW networks, respectively. The DFOM images (Figure 2A & B) show the color of light scattered from the nanowires changes from reddish-orange to slightly neutral gray upon coating with Pt. The electroplating of Pt occurred only on the surface of the Cu NWs, with no platinum deposited on the open area of the substrate. This allows the network to retain its transmittance after electroplating. The SEM images (Figure 2C & D) also show no particles were deposited on the glass, consistent with the DFOM images. In addition, the surface roughness of the NWs increases after Pt electroplating. Figure S2 shows this roughness increases slightly with electroplating time. TEM images (Figure

This journal is © The Royal Society of Chemistry 2014

Energy Environ. Sci., 2014, **00**, 1-7 | **3**

2E&F) also reveal an increase in surface roughness after Pt electroplating, as well as the nanocyrstalline nature of the Pt coating. EDS mapping (Figure 2G-I) shows the copper nanowire is completely coated with a thin layer of platinum. The average diameter of the Cu NWs is 70 ± 10 nm, and this increases to 84 ± 12 nm after electrodeposition of 9 mol% Pt to give an average shell thickness of 7 ± 2 nm. Further evidence for the complete coating of the Cu NWs with Pt at 9 mol% is demonstrated by the oxidation data shown in Figure S3. Cu NWs become nonconductive over a period of 5 days when stored in an oven at 85 °C, but the Cu NWs coated with 9 mol% Pt exhibit almost no change in conductivity over one month.[24]
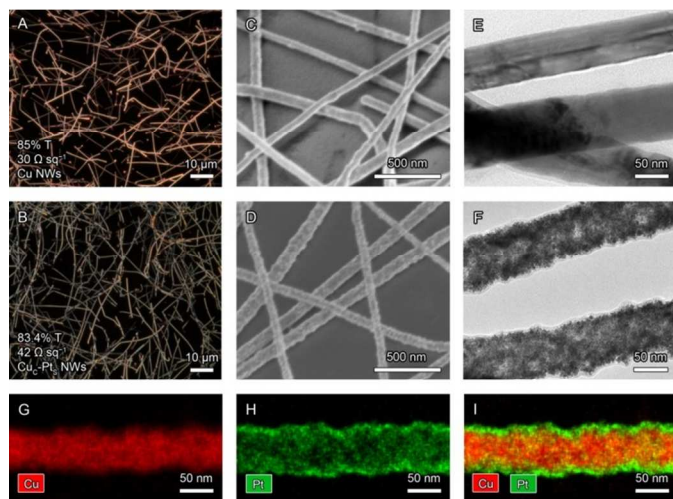

Figure 2. DFOM (A,B), SEM (C,D), and TEM (E,F) images of Cu NWs (A,C,E) and Cu_c-Pt_s (9 mol% Pt) NWs (B,D,F). (G−I) EDS mapping of a Cu_c-Pt_s (9 mol% Pt) NW.

X-ray photoelectron spectroscopy (XPS) was used to characterize the compositional and electronic changes caused by electrodeposition of Pt onto the Cu NWs (as well as after sustained hydrogen evolution and electroless plating of Pt, to be discussed later). Figure 3A shows Cu NWs exhibit two dominant peaks at 931.5 and 951.4 eV, characteristic of the $2p_{3/2}$ and $2p_{1/2}$ binding energies of Cu(0) metal, respectively.[25] The small rounded peaks at 943.6 and 962.0 eV can be attributed to CuO that results from surface oxidation of the Cu NWs. After electroplating the Cu NWs with Pt, the intensity of Cu(0) $2p_{3/2}$ and $2p_{1/2}$ peaks dropped by ~4 times, and two new peaks corresponding to Pt(0) $4f_{7/2}$ and $4f_{5/2}$ appeared at 70.7 and 74.0 eV, respectively (Figure 3B).[25] The small rounded peaks between 72 - 78 eV for Cu NWs can be attributed to the Cu(0) 3p doublet;[26] these peaks disappear after Pt coating. The fact that the Pt(0) 4f peak positions coincide with that of a polycrystalline Pt foil (purple curve in Figure 3B) indicate there is little effect of the Cu NW substrate on the electronic properties of the coated Pt. This is likely due to a lack of significant alloying between Cu and Pt after electrodeposition at room temperature.[27,28]
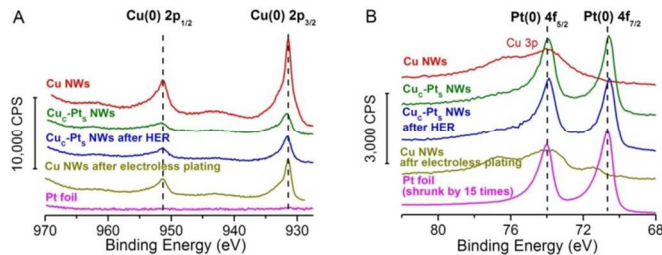

Figure 3. (A) Cu 2p and (B) Pt 4f XPS spectra of the Cu NWs, Cu_c-Pt_s NWs before and after water reduction, the Cu NWs after electroless plating, and a Pt foil.

Electrocatalytic Water Reduction. Figure 4A shows CVs obtained with Cu NW and Cu_c-Pt_s NW (9 mol% Pt) electrodes in 0.2 M deaerated phosphate buffer (pH 7.0). In the absence of a Pt coating, only a relatively small amount of hydrogen evolved at −0.75 V *vs.* NHE. With a Pt coating on the Cu NWs, the onset potential of hydrogen evolution occurs at approximately −0.42 V, which coincides with the standard electrode potential of hydrogen evolution (−0.41 V) at the pH used in the experiment. During the reverse scan, an anodic peak appears due to the re-oxidation of H_2 generated in the forward scan. The current response of the Cu_c-Pt_s (9 mol% Pt, 2.0 µg cm^{-2} of Pt) NW film is at least five times higher than that obtained for Pt/C with the same area coverage of Pt (2.0 µg cm^{-2}) under identical solution conditions.

The Cu_c-Pt_s NW film electrode was used for controlled potential electrolysis at −0.65 V in 0.2 M deaerated phosphate buffer (pH 7.0). We chose this pH due to its relevance to artificial photosynthesis with water from natural sources.[7] Figure 4B shows the electrolysis proceeds with a stable current density level of ~1.15 mA/cm^2 for 6 h. XPS data in Figure 3 show no change in the Cu or Pt peaks after HER, further demonstrating their electrochemical stability. The Cu_c-Pt_s NWs were intact after HER (Figure S4), and the film maintained excellent optical (85.5%) and electrical (45 Ω sq^{-1}) performance. Electrolysis with the Cu_c-Pt_s NW film produced 6.45 µmol of H_2 over 6 h, with a Faradaic efficiency of 96%.

The current density of HER depends on both the Pt loading and the areal density of NWs. Figure 4C shows that the catalytic current density for the Cu_c-Pt_s network (Cu NW loading 65 mg/m^2) in 0.2 M deaerated phosphate buffer (pH 7.0) increases with Pt content up to approximately 10 mol%, again suggesting that complete surface coverage of Pt on the Cu NWs is obtained at this mol%. The current density per microgram of platinum is highest at the lowest loading of Pt on the Cu NWs, reaching a value of 1.45 mA cm^{-2} µg^{-1} at 2.5 mol%, about 8 times greater than the value obtained for Pt/C. The current density per microgram of platinum approaches that of Pt/C at a platinum loading of > 20 mol%.

The catalytic current density of the Cu_c-Pt_s network could be further enhanced by increasing the density of nanowires on the substrate. As shown in Figure 4D, the current density increases linearly with the NW loading. A current density of 1.70 mA/cm^2 was achieved by increasing the areal density of Cu NWs to ~100 mg m^{-2} (9 mol% Pt, < 15 Ω sq^{-1}, 77% at 550 nm). This current density is comparable to an activity of 1.80 mA/cm^2 for a polycrystalline Pt foil under the same experimental conditions. The trend in Figure 4D suggests an even higher catalytic current density can be attained at the expense of film transmittance.
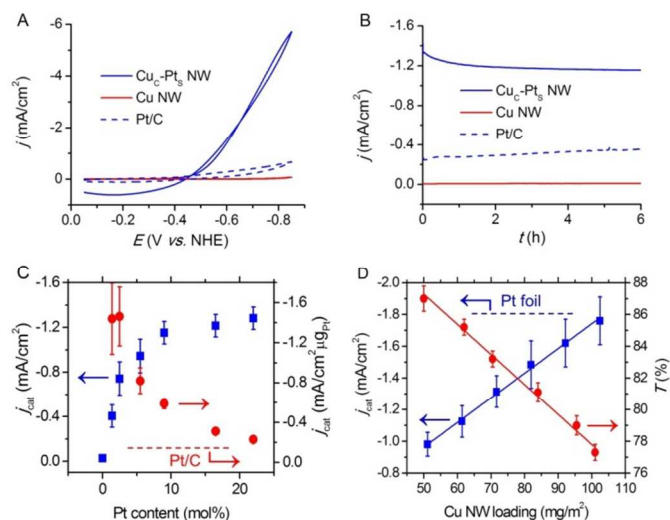
4 | *Energy Environ. Sci.*, 2014, **00**, 1-7

This journal is © The Royal Society of Chemistry 2014

Figure 4. (A) Cyclic voltammograms (100 mV/s) and (B) controlled potential electrolysis (−0.65 V *vs.* NHE) for the Cu and Cu$_c$-Pt$_s$ (9 mol% Pt) NW networks in 0.2 M deaerated phosphate buffer (pH 7.0). For comparison, the dashed lines show the cyclic voltammograms and controlled potential electrolysis obtained with Pt/C on ITO, using the same amount of Pt (2.0 μg cm^{-2}). (C) Plots of catalytic current density (−0.65 V) and Pt-mass normalized catalytic current density (−0.65 V) *vs.* Pt content for the HER. (D) Plots of catalytic current density (−0.65 V) and transmittance (550 nm) of Cu NW network *vs.* Cu NW loading.

Comparison with ITO. Figure 5 shows that the transparency of the Cu and Cu$_c$-Pt$_s$ NW films exceed that of ITO at wavelengths < 400 nm and > 1100 nm. The high transparency in the infrared region is potentially of importance, for example, for solar fuel production driven by infrared light.[29,30] About 40% of the solar energy reaching Earth's surface lies in the near-infrared region of the electromagnetic spectrum.[31] The ITO film has an average transmittance (λ = 300-1800 nm) of 74.4%, compared to 85.6% for Cu NWs and 84.6% for the Cu$_c$-Pt$_s$ NW film. In addition, the ITO film largely loses its transmittance in a reducing environment due to the reduction of In(III) oxide.[12] The reduction of ITO at −0.80 V *vs.* NHE for only 2 h decreased the average transmittance of ITO from 74.4% to 47.5%. The time-dependent decrease in the transmittance of ITO at −0.80 V is shown in Figure S5. In contrast, the transmittance of the Cu$_c$-Pt$_s$ (9 mol% Pt) NW network retained an average transmittance of 85.1% after reduction under the same experimental conditions. These results suggest that Cu$_c$-Pt$_s$ NWs are a robust, high-performance alternative to ITO for use in PECs, DSSCs, as well as spectroelectrochemical studies in electrochemically reductive environments.
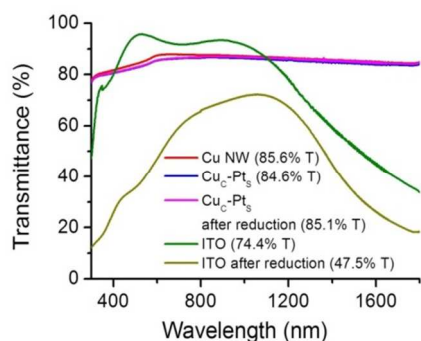

Figure 5. Plots of specular transmittance *vs.* wavelength for Cu NWs, Cu$_c$-Pt$_s$ NWs (9 mol% Pt) before and after reduction at −0.80 V *vs.* NHE for 2 h, and ITO before and after reduction at −0.80 V *vs.* NHE for 2 h. The transmittance data labeled in the figure are averaged over λ = 300-1800 nm.

Electroplating vs. Galvanic Replacement. Cu NWs coated with Pt have previously been produced by partial galvanic replacement of Cu NWs 100 nm in diameter with Pt in a solution of H$_2$PtCl$_6$.[17,18] Galvanic replacement etches the Cu NWs, leading to a reduction in their length due to breakage, and the eventual formation of Pt nanotubes.[19] As we will show, galvanic etching increases the resistance of the nanowires, making them unsuitable for use as an electrode on their own. Indeed, previous studies did not perform sheet resistance or transmittance measurements on films of Cu$_c$-Pt$_s$ NWs. Instead, the nanostructures were deposited from solution onto working electrodes made from glassy carbon, and coated with Nafion to bind them to the substrate.

To provide a direct comparison of electroplating with galvanic replacement, we immersed a Cu NW film in a 0.2 M deaerated phosphate buffer (pH 7.0) containing 0.1 mM K$_2$PtCl$_6$ (the same solution used for electroplating). After 10 min, the transmittance of the film increased from 85% to 87 - 88%, and the sheet resistance increased from 32 Ω sq^{-1} to 10^2 - 10^3 Ω sq^{-1}. This decrease in conductivity is likely due to galvanic etching of the Cu NWs, which results in the removal of two Cu atoms for every one Pt atom added to the NWs. Figure S6A shows the Cu NW film largely retained its copper color at 10 min, suggesting little Pt was deposited. The XPS in Figure 3B shows only a small Pt signal from this film. The CV of the film in Figure S6C shows there is some catalytic current enhancement relative to Cu NWs, but it is 50 times less than that obtained with the Cu$_c$-Pt$_s$ nanowires coated with 9 mol% Pt by electroplating over 10 min. Extending the immersion time to 60 min caused additional etching of the CuNWs and their disappearance from the substrate, giving the film a transmittance of 90-93% at 550 nm and a sheet resistance of > 10^5 Ω sq^{-1} (Figure S6B). Thus, galvanic replacement is clearly inferior to electroplating in its ability to deposit Pt onto the Cu NWs while retaining the conductivity of the nanowires. The fact that electrodeposition of Pt results in relatively little etching of the Cu NWs compared to galvanic replacement allowed us to use the Cu$_c$-Pt$_s$ NWs as an electrocatalyst directly for the first time, without the need for a conductive substrate or a coating of Nafion or other binding agents that may occupy the active sites of the catalyst. This fabrication method can likely be extended to create core–shell nanowire networks by electroplating ions of other noble metals (*i.e.*, Au and Pd) that would otherwise etch the copper nanowires.[19]

Extension to a Flexible Substrate. We also produced and examined the properties of Cu$_c$-Pt$_s$ NW networks on polyethylene terephthalate (PET), a plastic substrate widely used for flexible, transparent conductive films. As shown in Figures S7 & S8, the electroplating of Pt onto Cu NWs and the catalytic activity of Cu$_c$-Pt$_s$ NW networks toward hydrogen evolution is virtually the same on PET as it is on glass. Cu NW films on PET were previously bent 1000 times with little degradation in sheet resistance (30 Ω sq^{-1} to 40 Ω sq^{-1}).[15] To confirm that the flexibility is retained after Pt electroplating, a Cu$_c$-Pt$_s$ NW (9 mol% Pt) film was repeatedly bent from a 10 mm to a 2.5 mm radius of curvature. Figure 6 shows the sheet resistance of the film increased slightly from 42 to 140 Ω sq^{-1} (~2.5 times of increase) after 1000 bends. The flexibility of the Cu$_c$-Pt$_s$ NW (9 mol% Pt) film is also retained after sustained hydrogen

This journal is © The Royal Society of Chemistry 2014

Energy Environ. Sci., 2014, **00**, 1-7 | **5**

evolution. This is in contrast to the ITO film on PET, for which the sheet resistance increased by 400 times after just 250 bends. Considering the low cost and design flexibility of transparent plastics compared to glass, the extension to plastic substrates could enable new, versatile, and lower cost design architectures for solar fuel devices.
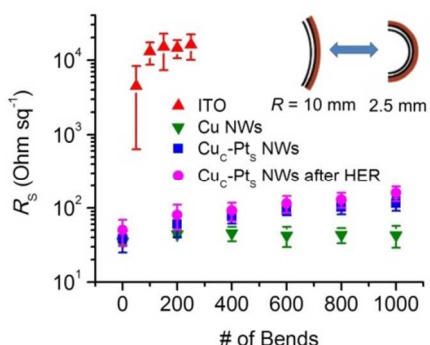

Figure 6. Plots of sheet resistance (R_S) vs. number of bends for films of ITO, Cu NWs, and Cu_c-Pt_s (9 mol% Pt) NWs before and after sustained hydrogen evolution on PET.

Conclusions

This study has reported the first fabrication and use of a transparent, conducting electrocatalyst composed of a film of Cu_c-Pt_s nanowires. A Pt content of 9 mol% was sufficient to completely coat the copper nanowires, as indicated by their stability to oxidation, and the maximum in the HER current density vs. Pt loading. The highest mass activities (8 times that of Pt/C) were obtained at the lowest loading of Pt on the Cu NWs (< 3 mol%). The networks of Cu_c-Pt_s NWs could achieve current densities comparable to a polycrystalline Pt foil while retaining a transmittance of > 75%, suggesting that current densities greater than those from Pt foil can be obtained at higher loadings (> 100 mg/m^2) of nanowires on the substrate. The electrochemical stability of Cu_c-Pt_s NW films allows them to retain a high transmittance (85.1%, averaged over λ = 300-1800 nm) after electrochemical reduction. In contrast, the transmittance of an ITO film drops from 74.4% to 47.5% under the same conditions. The optoelectronic performance of the NW film can be further improved through the use of Cu NWs with higher aspect ratios (L/D).[32] In conclusion, the excellent electrochemical stability, tunable electrical conductivity, broadband transparency, mechanical flexibility, and electrocatalytic performance of films of Cu_c-Pt_s NWs make them an attractive alternative to ITO-supported catalysts for photoelectrochemical cells, dye sensitized solar cells, and spectroelectrochemistry.

Acknowledgements

Notes and references

1 M. G. Walter, E. L. Warren, J. R. McKone, S. W. Boettcher, Q. Mi, E. A. Santori, N. S. Lewis, *Chem. Rev.*, 2010, **110**, 6446−6473.
2 T. R. Cook, D. K. Dogutan, S. Y. Reece, Y. Surendranath, T. S. Teets, D. G. Nocera, *Chem. Rev.*, 2010, **110**, 6474−6502.
3 N. P. Dasgupta, C. Liu, S. Andrews, F. B. Prinz, P. Yang, *J. Am. Chem. Soc.*, 2013, **135**, 12932−12935.
4 D. Gust, T. A. Moore, A. L. Moore, *Acc. Chem. Res.*, 2009, **42**, 1890−1898.
5 M. Grätzel, *Nature*, 2001, **414**, 338−344.
6 J. H. Alstrum-Acevedo, M. K. Brennaman, T. J. Meyer, *Inorg. Chem.*, 2005, **44**, 6802−6827.
7 S. Y. Reece, J. A. Hamel, K. Sung, T. D. Jarvi, A. J. Esswein, J. J. H. Pijpers, D. G. Nocera, *Science*, 2011, **334**, 645−648.
8 Z. Chen, A. R. Rathmell, S. Ye, A. R. Wilson, B. J. Wiley, *Angew. Chem. Int. Ed.*, 2013, **52**, 13708-13711.
9 N. S. Lewis, D. G. Nocera, *P. Natl. Acad. Sci. U.S.A.*, 2006, **103**, 15729−15735.
10 M. Aparicio, A. Jitianu, L. C. Klein, *Sol-Gel Processing for Conventional and Alternative Energy*, page 286; Springer New York Heidelberg Dordrecht London, 2012.
11 U.S. Geological Survey, *Mineral Commodity Summaries. Indium*, 2011, 74.
12 P. M. S. Monk, C. M. Man, *J. Mater. Sci.: Mater. Electron.*, 1999, **10**, 101−107.
13 U.S. Geological Survey, *Mineral Commodity Summaries. Copper*, 2011, 48.
14 H. Z. Guo, N. Lin, Y. Z. Chen, Z. W. Wang, Q. S. Xie, T. C. Zheng, N. Gao, S. P. Li, J. Y. Kang, D. J. Cai, D. L. Peng, *Sci. Rep.*, 2013, DOI: 10.1038/srep02323
15 A. R. Rathmell, B. J. Wiley, *Adv. Mater.*, 2011, **23**, 4798−4803.
16 A. V. Ruban, H. L. Skriver, J. K. Nørskov, *Phys. Rev. B*, 1999, **59**, 15990−16000.
17 S. M. Alia, K. Jensen, C. Contreras, F. Garzon, B. Pivovar, Y. Yan, *ACS Catal.*, 2013, **3**, 358−362.
18 S. M. Alia, B. S. Pivovar, Y. Yan, *J. Am. Chem. Soc.*, 2013, **135**, 13473−13478.
19 X. F. Lu, M. McKiernan, Z. M. Peng, E. P. Lee, H. Yang, Y. N. Xia, *Sci. Adv. Mater.*, 2010, **2**, 413−420.
20 L. Kavan, J. H. Yum, M. Grätzel, *ACS Nano*, 2011, **5**, 165−172.
21 H. Yang, *Angew. Chem. Int. Ed.*, 2011, **50**, 2674−2676.
22 A. Heller, D. E. Aspnes, J. D. Porter, T. T. Sheng, R. G. Vadimsky, *J. Phys. Chem.*, 1985, **89**, 4444−4452.
23 J. Lewis, *Mater. Today*, 2006, **9**, 38−45.
24 P.-C. Hsu, H. Wu, T. J. Carney, M. T. McDowell, Y. Yang, E. C. Garnett, M. Li, L. Hu, Y. Cui, *ACS Nano*, 2012, **6**, 5150−5156.
25 C. D. Wanger, W. M. Riggs, L. E. Davis, J. F. Moulder, G. E. Muilenberg, in *Handbook of x-ray photoelectron spectroscopy: a reference book of standard data for use in x-ray photoelectron spectroscopy*, Perkin-Elmer Corp., Physical Electronics Division, Eden Prairie, Minnesota, USA, 1979, pp. 78−82.
26 R. Hesse, P. Streubel, R. Szargan, *Surf. Interface Anal.*, 2005, **37**, 589−607.
27 A. Sarkar, A. Manthiram, *J. Phys. Chem. C*, 2010, **114**, 4725−4732.
28 C. J. Corcoran, H. Tavassol, M. A. Rigsby, P. S. Bagus, A. Wieckowski, *J. Power Sources*, 2010, **195**, 7856−7879.
29 J. Tang, E. H. Sargent, *Adv. Mater.*, 2011, **23**, 12−29.
30 F. Odobel, L. Le Pleux, Y. Pellegrin, E. Blart, *Acc. Chem. Res.*, 2010, **43**, 1063−1071.

31 Q. Fu, **2003**, *Radiation (Solar);* In J. R. Holton, *Encyclopedia of atmospheric sciences Vol. 5 [Rad - S]*. Amsterdam: Academic Press. pp. 1859–1863.

32 S. Ye, A. R. Rathmell, I. E. Stewart, Y.-C. Ha, A. R. Wilson, Z. Chen, B. J. Wiley, *Chem. Commun.*, 2014, **DOI:** 10.1039/C3CC48561G.

This journal is © The Royal Society of Chemistry 2014

Energy Environ. Sci., 2014, **00**, 1-7 | **7**

Energy & Environmental Science

ARTICLE

Table of Contents